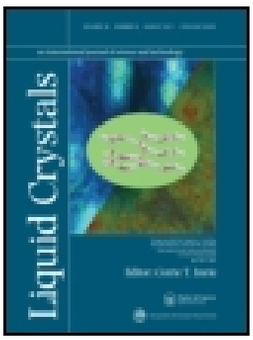

Liquid Crystals

ISSN: (Print) (Online) Journal homepage: https://www.tandfonline.com/loi/tlct20

Fringe-field-induced out-of-plane reorientation in vertically aligned nematic spatial light modulators and its effect on light diffraction

Inge Nys, Jeroen Beeckman & Kristiaan Neyts

To cite this article: Inge Nys, Jeroen Beeckman & Kristiaan Neyts (2021): Fringe-field-induced out-of-plane reorientation in vertically aligned nematic spatial light modulators and its effect on light diffraction, Liquid Crystals, DOI: 10.1080/02678292.2021.1881831

To link to this article: https://doi.org/10.1080/02678292.2021.1881831

Published online: 12 Mar 2021.

LIQUID CRYSTALS
https://doi.org/10.1080/02678292.2021.1881831

Taylor & Francis
Taylor & Francis Group

Fringe-field-induced out-of-plane reorientation in vertically aligned nematic spatial light modulators and its effect on light diffraction

Inge Nys, Jeroen Beeckman and Kristiaan Neyts

LCP Group, Department of Electronics and Information Systems, Ghent University, Ghent, Belgium

ABSTRACT

Liquid crystal (LC)-based spatial light modulators (SLMs) have the ability to shape the wavefront of a light beam and are widely used in applications where phase or amplitude modulation is required. In this work we study the LC director configuration in vertically aligned nematic (VAN) SLMs, with a focus on 1D binary gratings with different driving voltages. By comparing experimental microscopy measurements with simulations, we demonstrate that the director can rotate out of the plane determined by the pretilt of the SLM. By twisting out of the pretilt plane, the formation of a reverse tilt zone in the LC director configuration is avoided. The twist effect is asymmetric and only occurs at the edges where the fringe-field of the high voltage pixel is inclined in the same direction as the pretilt. Due to the out-of-plane reorientation of the director at one side of the pixel, binary gratings show strongly asymmetric diffraction in the pretilt plane. The out-of-plane reorientation also induces changes in the polarisation state of the light beam and the competition between two different out-of-plane reorientation directions may lead to slow switching. It is therefore of utmost importance to consider this effect when using VAN SLMs in applications.

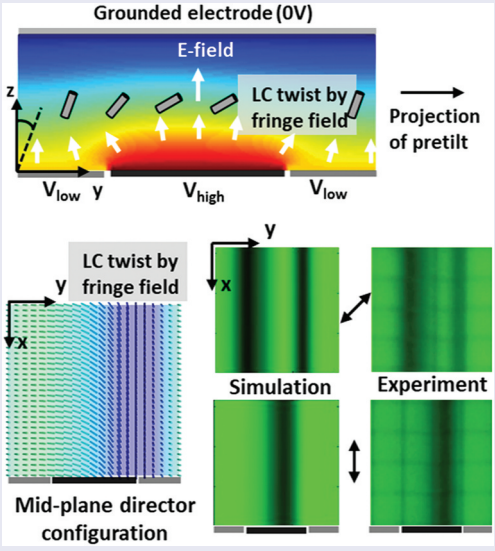

ARTICLE HISTORY
Received 13 November 2020
Accepted 23 January 2021

KEYWORDS
Spatial light modulator; liquid crystal; phase modulation; vertically aligned nematic; fringe-field; out-of-plane reorientation

I. Introduction

Liquid crystal (LC)-based spatial light modulators (SLMs) are reflective or transmissive components with a large number of electrically addressable pixels, that can locally and dynamically control the phase or the polarisation of light [1–15]. Wavefront shaping of a coherent beam by phase modulation is required in many rapidly developing applications including holographic optical trapping, holographic displays, solid-state light detection and ranging (LIDAR), virtual and augmented reality, etc. For phase modulation, the light that is incident on the SLM is polarised in the plane parallel to the pretilt of the LC [1–11]. Electrically addressed reorientation of the LC is also used in LC microdisplays based on amplitude modulation [16–19]. In this case, the polarisation of the incident light makes an angle of 45 degrees with the pretilt plane. The polarisation state of the light is modified and a polariser is used to obtain modulation of the

CONTACT Kristiaan Neyts Kristiaan.Neyts@Ugent.be

amplitude. Two decades ago the development of the liquid crystal on silicon (LCOS) technology was driven by the successful use of amplitude modulation in cinema projectors and rear projection TVs. Nowadays the technology is reviving in the form of phase modulating SLMs for structured light applications [1]. Customer demands are becoming more and more stringent, requiring SLMs with ever increasing resolution and switching speed [1,5–7]. However, with the decrease in pixel dimensions, the cross-talk between neighbouring pixels becomes more important and the phase retardation within the pixel area is increasingly non-uniform [2]. Especially in driving patterns with strong spatial variations, the inhomogeneity in each pixel can lead to a phase pattern that strongly deviates from the expected one. Moreover, the interaction between neighbouring pixels at different voltages can lead to an unwanted change in the polarisation, instead of the intended phase modulation.

We here consider vertically aligned nematic (VAN) SLMs with a small pretilt (θ_P = 3°) towards the +y direction as illustrated in Figure 1. For phase modulation, light polarised along the y-axis is incident perpendicularly onto the SLM (along the z-axis). As long as the LC director remains in the yz-plane (the plane spanned by the pretilt and the substrate normal), the polarisation

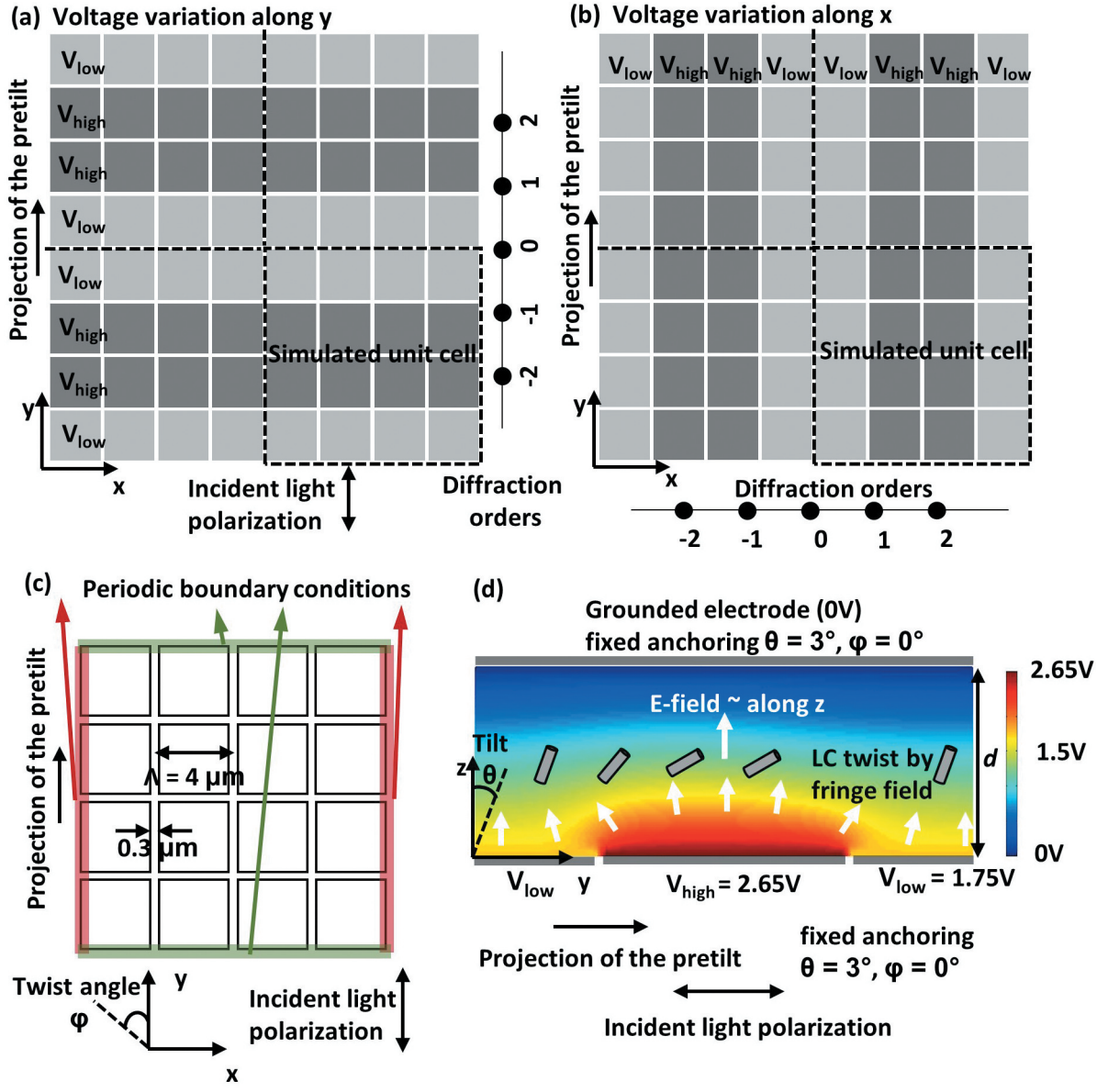

Figure 1. Top view (xy-plane) of the VAN SLM with rows of equal voltage (a) and columns of equal voltage (b). The simulated unit cell is enlarged in (c). Vertical cross-section (yz-plane) (d) with schematic presentation of the electric field lines for varying pixel voltages along the y-axis.

state of the light beam is unchanged and only the phase is modulated. However, when the voltage difference between neighbouring pixels introduces a twist of the LC director out of the yz-plane, also the polarisation state of the beam is affected. Polarisation change is an important loss factor for phase modulating SLMs and should be carefully evaluated to optimise the efficiency in demanding applications.

VAN SLMs use LC with negative dielectric anisotropy ($\Delta\varepsilon < 0$) on top of pixels on a silicon backplane. Upon application of an electric field, the LC preferentially orients the director in the plane perpendicular to the electric field lines. This is substantially different from LC with a positive dielectric anisotropy where the unique direction, parallel to the electric field lines, is preferred [16]. The uncertainty for the director in LC with $\Delta\varepsilon < 0$ to rotate in a particular direction, can to some extent, be lifted by the pretilt in the anchoring at the surface. However, in this work we demonstrate that an out-of-plane twist (out of the yz-plane) of the director can occur between neighbouring pixels in VAN SLMs, also when there is a voltage variation along the y-axis (case (a) in Figure 1). An existing hypothesis explains that, close to these transitions where the fringe-field is inclined in the same direction as the pretilt, a so-called reverse tilt zone can exist where the LC molecules tilt towards the – y axis (opposite to the rest of the pixel) [18–20]. We here show that another deformation of the LC director occurs, where conflicting torques due to the anchoring pretilt and the fringe-field close to the interpixel gap lead to an out-of-plane reorientation of the director. In this way, the total free energy, containing elastic and electric energy terms, can be minimised. This out-of-plane reorientation of the director has far-reaching implications for the proper operation of the SLM device: it changes the phase delay, the polarisation of the reflected light and the switching dynamics. Two possible out-of-plane reorientation directions (towards +x or – x direction) exist and result in a bistability or slow switching, depending on the driving history of the SLM.

In this work, the voltage-induced director reorientation in VAN SLMs is studied for different voltage combinations between neighbouring pixels, based on experiments and numerical simulations. The simulation results for the LC director are reported in section II and the simulated optical transmission is compared to microscopy images in section III. The effect on the far-field diffraction characteristics is commented upon in section IV and the switching between binary column gratings and row gratings is discussed in section V.

II. Numerical simulation of the director configuration

A finite element Q-tensor model is used to simulate the director configuration in an SLM with a cell thickness d of 3 μm, a pixel pitch Λ of 4 μm and an electrode gap of 0.3 μm between neighbouring pixels [21,22]. A pixel pitch of 4 μm is typical for state of the art high-resolution phase modulators and a 3 μm thick layer thickness is common for phase modulators working in the visual wavelength range [2,3,16,20]. Details of the simulation method, developed at University College London, can be found in previous references [21–26]. Strong anchoring is assumed at the alignment surfaces (fixed directors at z = 0 and z = d) and periodic boundary conditions are applied in the lateral directions (Figure 1). The effect of an applied root-mean-squared voltage on the pixel electrodes is simulated, without taking into account multiplexed sequences of high and low voltages that are typically used in applications. The LC parameters (dielectric anisotropy $\Delta\varepsilon$, refractive index contrast Δn and elastic constants K_{11}, K_{22} and K_{33}), anchoring conditions (pretilt angle θ_P) and cell thickness (Table 1) are roughly estimated based on comparison between experimental results and simulations (uniform voltage vs. retardation curve), and common values reported in the literature [2,10,20]. The experimentally measured SLM supports phase modulation gratings with UHD resolution (3840 x 2160), has a reflective back contact, is designed for green light and has a maximum experimentally measured double pass phase retardation $\Gamma = (4\ \pi\ \Delta n\ d)/\lambda \approx 2.55\ \pi$ for $\lambda = 532$ nm. Details about the type of LC material used in the SLM are not disclosed by the supplier. Although the exact choice for the simulation parameters slightly influences the results, the general conclusions and insights in the VAN SLM behaviour remain valid. Similar results were obtained for somewhat adjusted cell thickness, pretilt angle, dielectric anisotropy, refractive index contrast and elastic constants.

For simplicity, binary (on/off) gratings are considered and the equilibrium director configuration is simulated for four different voltage combinations (V_{low}, V_{high}) at the bottom pixel electrodes: (1.75 V, 2.2 V) (1.75 V, 2.35 V), (1.75 V, 2.65 V) and (2.35 V, 3.6 V). The counter electrode at the top surface is grounded (0 V) and all pixel voltages

Table 1. Simulation parameters.

Pixel pitch Λ	4 μm	K_{11}	11.1 pN	n_o	1.52	ε_{low}	6
Thickness d	3 μm	K_{22}	6.5 pN	n_e	1.67	ε_{high}	10
Interpixel gap	0.3 μm	K_{33}	13 pN	θ_P	3°		

are above the Fréedericksz threshold. For uniform driving of the SLM (with the same voltage applied to all pixels), the voltages 1.75 V, 2.2 V, 2.35 V, 2.65 V and 3.6 V correspond to a double pass (propagating back and forth through the LC layer) phase retardation $\Gamma = (4\,\pi\,\Delta n\,d)/\lambda$ for green light λ = 532 nm of respectively 0.14 π, 0.77 π, 1.0 π, 1.37 π and 2.07 π. We focus on binary gratings with two neighbouring rows (or columns) of pixels at a high voltage V_{high} and two rows (or columns) of neighbouring pixels at a low voltage V_{low} as shown in Figure 1 (a) (or Figure 1 (b)).The simulated and experimentally measured gratings have a period corresponding to four times the pixel pitch 4Λ = 16 µm.

Figure 2 shows the simulated equilibrium director configuration for gratings with rows or columns of equal voltages, for the four different voltage combinations (V_{low}, V_{high}). Remarkable results for the director configuration are found in the gratings with rows of equal voltage (Figure 2 Row-1, Row-2, Row-3, Row-4). When the voltage difference between neighbouring

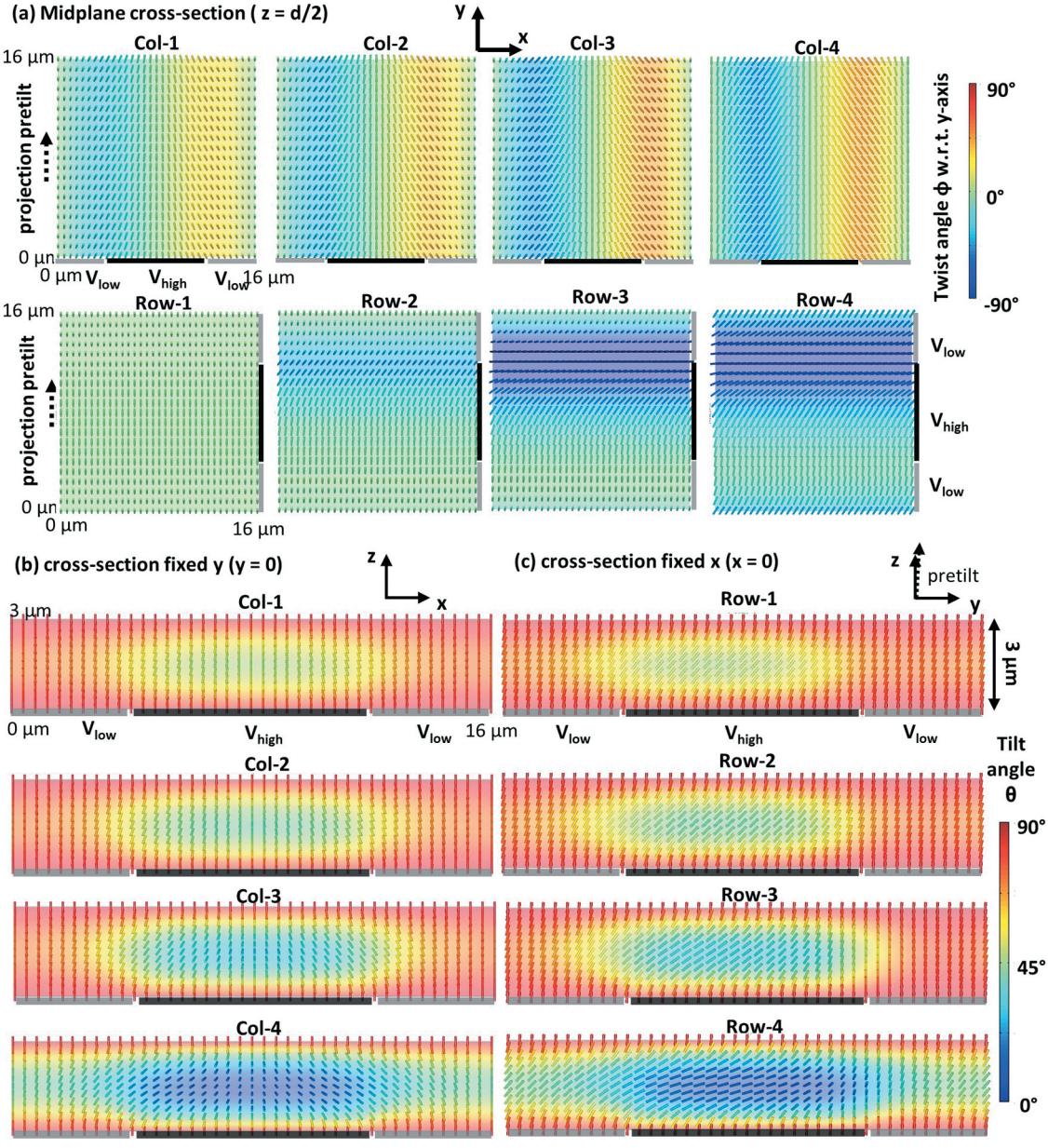

Figure 2. Simulated director configuration for gratings with columns of equal voltage (Col) and rows of equal voltage (Row), with different applied voltages V_{low} and V_{high}. Indices 1, 2, 3 and 4 stand for voltage combination (V_{low}, V_{high}) = (1.75 V, 2.2 V) (1.75 V, 2.35 V), (1.75 V, 2.65 V) and (2.35 V, 3.6 V). For all gratings the midplane cross-section (z = d/2) is shown in (a) with a colour representation for the twist angle φ. A cross-section for fixed y (b) and for fixed x (c) with the colour representing the tilt angle θ for column or row gratings.

electrodes in these gratings is large enough -for all cases, except for (1.75 V, 2.2 V) in the simulated examples- the director rotates out of the yz-plane (Figure 2 (a)), near the pixel edge where the voltage goes from high to low in the direction of the pretilt. At this transition, corresponding to the upper edge of the rows with V_{high} applied in Figure 2, the fringe-field is inclined in the same direction as the pretilt. This out-of-plane twist can occur in two equivalent directions (towards +x or – x) and only one of the two possible solutions is shown in Figure 2. An asymmetric phase retardation profile is expected, with the upward and downward transition between pixels at V_{high} and V_{low} being non-equivalent because of the presence of a non-zero pretilt. In the VAN SLM configuration with negative dielectric anisotropy, the retardation profile in these gratings is not only asymmetric, also an out-of-plane twist occurs near one of the two voltage transitions.

When a voltage is applied to the device in the initial 0 V state (all directors along the preferred pretilt direction), the field in the middle of the pixel is practically parallel to the z-axis, and the fringe fields near the horizontal edges of the pixels are tilted in the yz-plane (Figure 1 (d)). In the region where the tilt of the fringe field is larger than the pretilt of the director, the torque is in the positive x-direction, while in the rest of the pixel the torque is in the negative x-direction. The large elastic energy resulting from a tilt in the opposite directions (creating a so called reverse tilt zone [18–20],) can be reduced by introducing an out-of-plane twist (out of the yz-plane) in the director configurations. As can be seen in Figure 2, a larger voltage difference between neighbouring electrodes leads to a larger twist and a larger area with twist. It is clear that the region with an out-of-plane twist can extend over a large distance and disrupt the expected pixel response.

A director reorientation outside the yz-plane also occurs for gratings with columns of equal voltage, as shown in Figure 2 Col-1, Col-2, Col-3 and Col-4, but the origin and the consequences of this effect are different. The director twist is now symmetric for the two edges of the columns (to the left and to the right of the columns with V_{high}) and there is no threshold voltage for out-of-plane twist reorientation (Figure 2 (a)). The fringe electric fields are pointing away from the centre of the column with high voltage, and the LC director tilts towards the centre of this column, which is expected for a material with negative $\Delta\varepsilon$. In this case there is no slow switching dynamics and there are no competing domains. Out-of-plane reorientation occurs with the same unique twist direction along the full grating edge.

III. Optical transmission: simulation and experiment

Based on the simulated director configuration (as shown in Figure 2), the optical transmission for different orientations of the polariser is simulated with the help of the Jones Calculus for λ = 532 nm. 100% reflectivity of the back contact is assumed and both the incident and the reflected light pass through the same polariser. The resulting optical transmission (in reflection mode) at different driving levels is compared with experimental microscopy images in Figure 3. In the experiment, one polariser is placed on top of the reflective SLM, and the input light and the reflected light are passing through the same polariser. An area of 8 × 8 pixels is shown (with always two pixel-wide columns or rows at a voltage V_{high} and two pixel-wide columns or rows at V_{low}). Observations with the polariser oriented along the y-axis are used to identify out-of-plane reorientation effects. When the LC director reorients solely in the yz-plane, by changing its tilt angle but not its twist angle, the transmission should remain high in this case. Any out-of-plane reorientation of the director induces a change in the polarisation state when the light is propagating through the LC layer and will result in a lower transmission by the analyser. Also observations with the polariser oriented at 45° are shown, which roughly allow to monitor the induced phase retardation (although the out-of-plane twist also has an effect on the transmission). There is very good agreement between the experimental results and the simulation results in Figure 3, which clearly indicates that the LC configuration in the SLM (as discussed in section II) is correctly simulated for different voltage combinations.

IV. Simulation of the far-field diffraction characteristics

Proper understanding of the director configuration for different voltage combinations on the pixels is very important for the use of SLMs in practical applications. Pixel crosstalk and director twist near the edges can strongly modify the desired device response. When the SLM is used to deflect a light beam, the incident light is polarised along the y-axis, parallel to the pretilt plane. Due to the out-of-plane twist of the director, not only the phase delay of the light beam will be modulated but also the polarisation state will be changed. After reflection, in many applications the light is passing through a polariser that is parallel to the polarisation direction of the input beam. Out-of-plane reorientation of the director therefore constitutes a loss due to the change in the

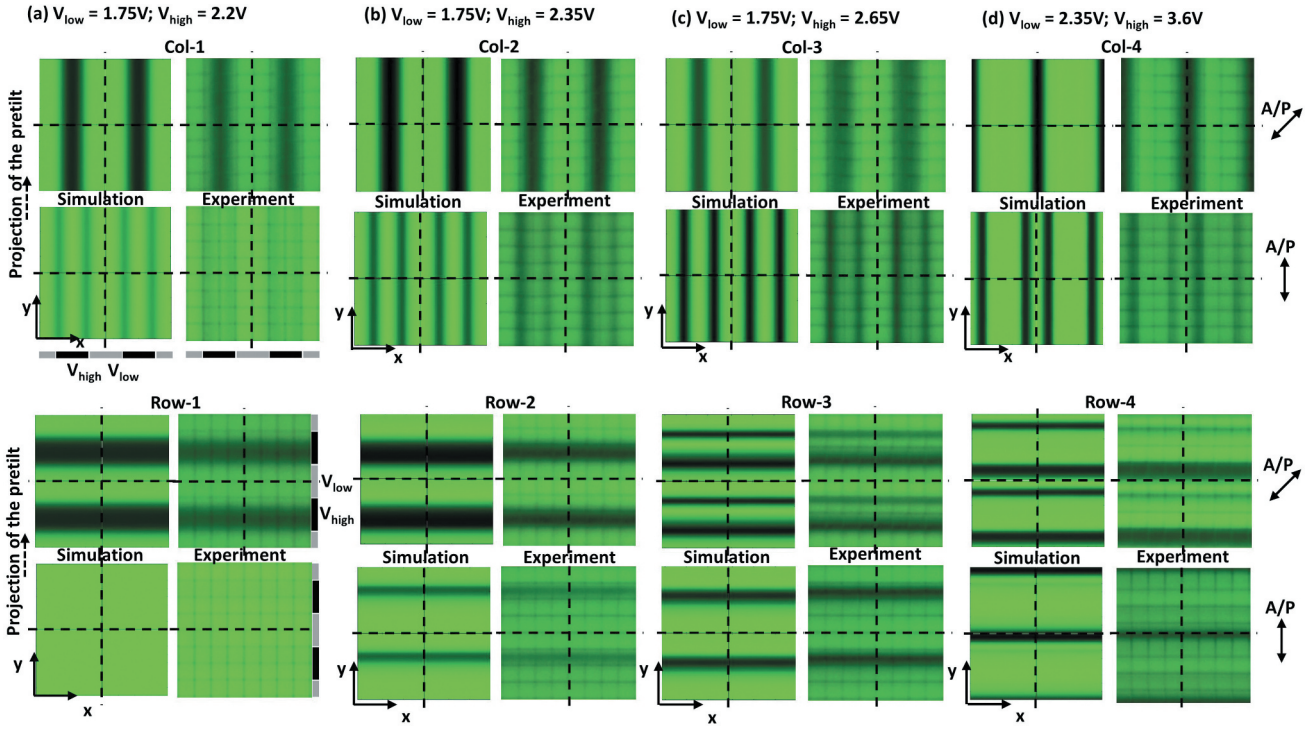

Figure 3. Simulated and experimentally measured optical microscopy images for 8 × 8 pixels, for gratings with columns (Col) and rows (Row) with equal voltages (alternating V_{low} and V_{high}) for two orientations of the polariser (along the y-axis and along the xy-diagonal). Simulations are performed for λ = 532 nm and a green filter was used in the experiments.

polarisation. Moreover, in gratings with rows of equal voltage and variable voltage in the pretilt (y) direction (Figure 1 (a)), the out-of-plane reorientation near one edge induces an asymmetry between the +1st and −1st diffraction order.

Based on the simulated results for the optical transmission with the Jones calculus (section III), far-field diffraction characteristics for linearly polarised light were found with the help of a Fourier transform. As mentioned before, 100% reflectivity of the back contact is assumed and both the incident and the reflected/diffracted light pass through the same polariser. Table 2 summarises the simulated intensities for the -1^{st} order, 0 order and $+1^{st}$ order diffraction (for λ = 532 nm) for gratings with rows or columns of equal voltage, assuming only y-polarised light is detected. The loss fraction, absorbed by the polariser, is also given. A visual representation of the data in Table 2 is shown in Figure 4.

The diffraction efficiencies are compared to the theoretically calculated diffraction efficiencies based on an idealised (pixelated) phase profile with constant phase over the area of the high and low voltage pixels, without change in polarisation. For this comparison, the phase for the pixels is fixed at the value obtained from uniform driving of the SLM (e.g. 1.75 V corresponds to Γ = 0.14 π etc.). The deviations between the theoretically expected diffraction efficiency and the simulated efficiency can be explained by two effects. The effect of pixel crosstalk in SLMs is well known: neighbouring pixels are influencing each other and the phase profile is smoothed and not uniform within the pixel area. This effect becomes stronger with decreasing pixel size, increasing SLM thickness and increasing voltage difference between neighbouring pixels. The other effect is the out-of-

Table 2. Simulated diffraction efficiencies for gratings with 2 pixel columns or rows with equal voltage, for λ = 532 nm and different drive levels (polariser along y). Absolute values (w.r.t. the incident light) are reported, neglecting losses at the glass interfaces and back contact. Col, Row and Theo respectively stand for column gratings, row gratings, and according to the theory (with constant phase retardation in each pixel). Indices 1, 2, 3 and 4 stand for voltage combination (V_{low}, V_{high}) = (1.75 V, 2.2 V) (1.75 V, 2.35 V), (1.75 V, 2.65 V) and (2.35 V, 3.6 V). The theoretical phase difference, based on the retardation for uniform driving, in case 1, 2, 3 and 4 is 0.63 π, 0.86 π, 1.23 π and 1.07 π.

	Col-1	Row-1	Theo-1	Col −2	Row-2	Theo-2
Order −1	20%	21%	28%	28%	38%	39%
Order 0	46%	58%	30%	17%	25%	5%
Order +1	20%	19%	28%	28%	19%	39%
Loss	13%	0%	0%	23%	13%	0%
	Col-3	Row-3	Theo-3	Col −4	Row-4	Theo-4
Order −1	29%	53%	36%	29%	29%	40%
Order 0	3%	10%	17%	6%	18%	1%
Order +1	29%	4%	36%	29%	13%	40%
Loss	34%	20%	0%	26%	22%	0%

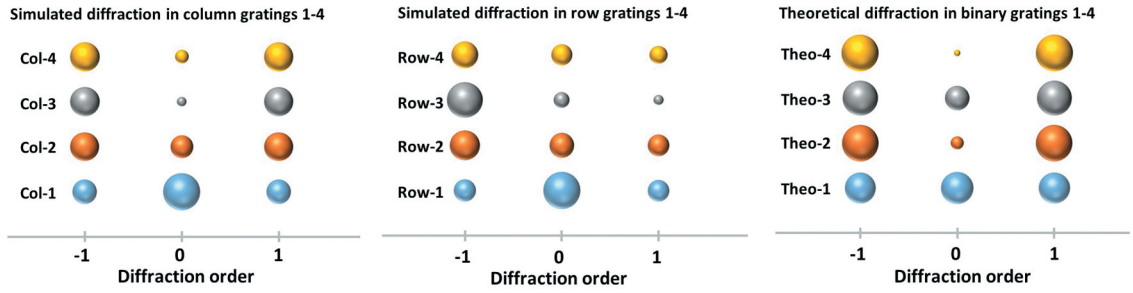

Figure 4. Visual representation of the diffraction efficiencies reported in Table 2. Simulated diffraction efficiencies for gratings with 2 pixel columns or rows with equal voltage, for λ = 532 nm and different drive levels (polariser along y). Col, Row and Theo respectively stand for column gratings, row gratings, and according to the theory (with constant phase retardation in each pixel). Indices 1, 2, 3 and 4 stand for voltage combination (V_{low}, V_{high}) = (1.75 V, 2.2 V) (1.75 V, 2.35 V), (1.75 V, 2.65 V) and (2.35 V, 3.6 V). The theoretical phase difference, based on the retardation for uniform driving, in situation 1, 2, 3 and 4 is respectively 0.63 π, 0.86 π, 1.23 π and 1.07 π.

plane twist of the director: this introduces loss by reducing the y-polarised component, which may also modify the distribution of light over the different diffraction orders.

For gratings with columns of equal voltage, symmetric diffraction with equal powers in the $+1^{st}$ and −1 order is observed for all driving levels (Table 2, Figure 4). The out-of-plane twist between pixels at different driving levels introduces a non-zero loss by changing the polarisation. Such a loss is also observed for gratings with rows of equal voltage, when the voltage difference between neighbouring pixels is sufficiently large (for all cases, except for (V_{low}, V_{high}) = (1.75 V, 2.2 V)). The results in Table 2 (Figure 4) illustrate that the diffraction for the gratings with rows of equal voltage is asymmetric, with a much higher efficiency for diffraction in the -1^{st} order than in the 1^{st} order. Symmetry breaking happens in these gratings because of the non-zero pretilt, and a certain asymmetry can be expected even when the director reorients only in the yz-plane (as in the example with (V_{low}, V_{high}) = (1.75 V, 2.2 V)). The out-of-plane reorientation of the director at the top side of the rows with V_{high} applied (from V_{high} to V_{low} along +y) makes the diffraction deviate much more form the theoretical prediction (Figure 4). The results for the binary grating with (V_{low}, V_{high}) = (1.75 V, 2.65 V) illustrate this: 53% of the light is diffracted in the −1st diffraction order while only 4% is diffracted in the +1st order. This example makes clear that detailed knowledge of the director configuration in the SLM is crucial to understand the operation of the device. Theoretical approximations, that only take into account smoothing of the phase retardation profile and asymmetry due to the pretilt, are not able to properly estimate the diffraction, if out-of-plane reorientation effects are neglected.

V. Switching from column gratings to row gratings

Finally, simulations are performed to better understand the switching behaviour between the two types of gratings. Figure 5 shows an intermediate director configuration (and corresponding polarised transmission images)

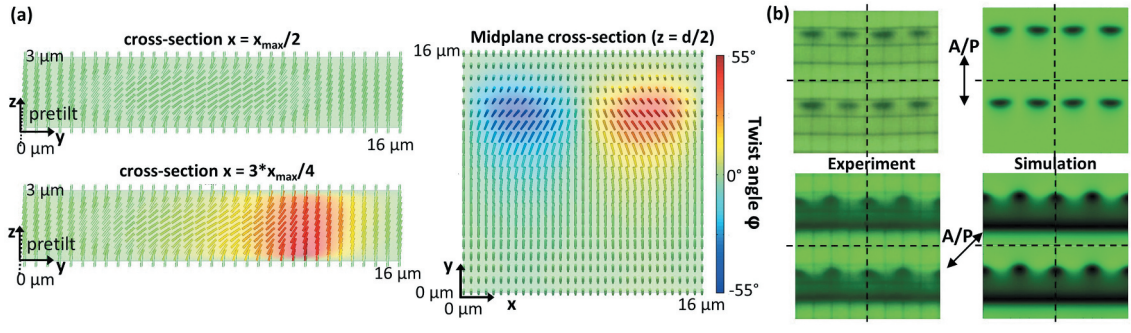

Figure 5. Intermediate configurations (0.2 s after switching) with two domains with different out-of-plane twist when switching from a column grating (Col-3) to a row grating (Row-3) (both with V_{low} = 1.75 V, V_{high} = 2.65 V). (a) simulated director configuration; (b) simulated and experimentally measured transmission for two different orientations of the polariser (along the y-axis and along the xy-diagonal).

that is obtained when switching from a grating with columns of equal voltage to a grating with rows of equal voltage, both with voltages V_{low} = 1.75 V and V_{high} = 2.65 V. As a result of the previously applied column gratings, two domains with different out-of-plane twist (towards +x and – x) are formed when the row pattern is applied. This configuration evolves towards a configuration that is invariant along the x-direction (Figure 2 Row-3) by preferred growth of the largest domain. Thanks to the symmetry in the structure, two final configurations with opposite out-of-plane twist can be formed with equal probability. Experimentally we observed a slow growth of the domains until the final configuration is reached. The growth rate can depend on the driving history, the applied voltage combination (V_{low}, V_{high}), the number of pixels in the grating, etc. A detailed study of the switching speed for different SLMs (different thickness, different LC, etc.), different voltage combinations and different grating patterns is outside the scope of this work, but our experimental observations indicate that switching times well above 1 second occur regularly. One of the main factors influencing the switching speed is the number of pixels in the grating. Switching between gratings with only a limited number of pixels (e.g. 1 or 2) in the grating period, is faster than switching between gratings with more pixels in the grating period.

VI. Conclusion

To conclude, in this article we experimentally measured and numerically simulated the LC director configuration in VAN SLMs for one-dimensional binary gratings with different driving voltages. The correspondence between microscopy images and numerical simulations of the optical behaviour confirms the validity of the simulation approach. We have, to our knowledge for the first time in VAN SLMs, demonstrated that an important out-of-plane reorientation of the LC director occurs near pixel edges that are perpendicular to the plane of the pretilt. This effect is asymmetric and only occurs at pixel edges where the fringe electric field is inclined in the same direction as the pretilt. This has a huge impact on the operation principle of the device: strongly asymmetric diffraction is observed in binary gratings, and very slow residual switching occurs when a grating with strong voltage variations in the direction of the pretilt is applied. These slow dynamics are related to the inherent bistability between two configurations with an opposite out-of-plane reorientation of the director. Initial switching, leading to changes in the phase retardation near the middle of the pixel, is fast but residual switching associated with the competition between different twist domains can be slow. In an ideal SLM with pretilt direction in the yz-plane, out-of-plane director reorientation towards the +x-axis and -x-axis is equally likely. In practice, a preference for one configuration may be induced by non-idealities such as a small deviation of the pretilt direction (at one or both substrates). It is very important to take into account the effects discussed in this article for future use of VAN SLMs in real-life applications.

Disclosure statement

No potential conflict of interest was reported by the author(s).

Funding

The work presented in this manuscript was funded by VLAIO - Flanders Innovation & Entrepreneurship [project HBC.2017.0141, MICROPRO].

References

[1] Lazarev G, Chen P-J, Strauss J, et al. Beyond the display: phase-only liquid crystal on silicon devices and their applications in photonics. Opt Express. 2019;27(11):16206–16249.
[2] Moser S, Ritsch-Marte M, Thalhammer G. Model-based compensation of pixel crosstalk in liquid crystal spatial light modulators. Opt Express. 2019;27(18):25046–25063.
[3] Chen H-MP, Yang J-P, Yen H-T, et al. Pursuing high quality phase-only liquid crystal on silicon (LCOS) devices. Appl Sci. 2018;8:2323.
[4] Zhang Z, You Z, Chu D. Fundamentals of phase-only liquid crystal on silicon (LCOS) devices. Light Sci Appl. 2014;3:e213.
[5] Li S-Q, Xu X, Veetil RM, et al. Phase-only transmissive spatial light modulator based on tunable dielectric metasurface. Science. 2019;364:1087–1090.
[6] Jin Y, Elston SJ, Fells JAJ, et al. Millisecond optical phase modulation using multipass configurations with liquid-crystal devices. Phys Rev Appl. 2020;14:024007.
[7] Feng Z, Ishikawa K. Phase modulator mode based on the pre-transitional effect of antiferroelectric liquid crystals. Opt Lett. 2018;43(2):251–254.
[8] Suchkov N, Fernandez EJ, Martinze-Fuentes JL, et al. Simultaneous aberration and aperture control using a single spatial light modulator. Opt Express. 2019;27(9):12399–12413.
[9] Xue S, Chen S, Tie G, et al. Adaptive null interferometric test using spatial light modulator for free-form sufaces. Opt Express. 2019;27(6):8414–8428.
[10] Fan-Chian K-H, Huang S-H, Shen C-Y, et al. Analog LCOS SLM devices for AR display applications. J Soc Inf Display. 2020;28:581–590.
[11] Garcia-Martinez P, Marco D, Martinez-Fuentes JL, et al. Efficient on-axis SLM engineering of optical vector modes. Opt Lasers Eng. 2020;125:105859.

[12] Beeckman J, Neyts K, Vanbrabant PJM. Liquid-crystal photonic applications. Opt Eng. 2011;50(8):081202 1–17.
[13] Maurer C, Jesacher A, Bernet S, et al. What spatial light modulators can do for optical microscopy. Laser Photon Rev. 2011;5(1):81–101.
[14] Dai Y, Antonello J, Booth MJ. Calibration of a phase-only spatial light modulator for both phase and retardance modulation. Opt Express. 2019;27(13):17912–17926.
[15] Runyon MT, Nacke CH, Sit A, et al. Implementation of nearly arbitrary spatially varying polarization transformations: an in-principle lossless approach using spatial light modulators. Appl Opt. 2018;57(20):5769–5778.
[16] Choi W-K, Hsu C-W, Tung C-H, et al. Effects of electrode structure and dielectric anisotropy on the performance of VA-FFS LC mode. Opt Express. 2019;27(23):34343–34358.
[17] Kumar P, Jaggi C, Sharma V, et al. Advancements of vertically aligned liquid crystal displays. Micron. 2016;81:34–47.
[18] Cuypers D, De Smet H, Van Calster A. Fringe field effects in microdisplays. SID05 Digest. 2005;36:1289–1301.
[19] Cuypers D, De Smet H, Van Calster A. Electronic compensation for fringe-field effects in VAN LCOS microdisplays. Sid 08 Digest. 2008;18:228–231.
[20] Vanbrabant PJM, Beeckman J, Neyts K, et al. Diffraction and fringing field effects in small pixel liquid crystal devices with homeotropic alignment. J Appl Phys. 2010;108(8):083104 1–6.
[21] James R, Willman E, Fernández FA, et al. Finite-element modeling of liquid-crystal hydrodynamics with a variable degree of order. IEEE Trans Electron Devices. 2006;53(7):1575–1582.
[22] Willman E, Fernández FA, James R, et al. Switching dynamics of a post-aligned bistable nematic liquid crystal device. J Display Technol. 2008;4(3):276–281.
[23] Nys I, Beeckman J, Neyts K. Switchable 3D liquid crystal grating generated by periodic photo-alignment on both substrates. Soft Matter. 2015;11(39):7802–7808.
[24] Nys I, Beeckman J, Neyts K. Surface-mediated alignment of long pitch chiral nematic liquid crystal structures. Adv Opt Mater. 2018;6(13):1800070.
[25] Nys I, Stebryte M, Ussembayev YY, et al. Tilted chiral liquid crystal gratings for efficient large-angle diffraction. Adv Opt Mater. 2019;7(22):1901364.
[26] Berteloot B, Nys I, Poy G, et al. Ring-shaped liquid crystal structures through patterned planar photo-alignment. Soft Matter. 2020;16(21):4999–5008.